ARTICLE NO. 79-0331R

Hot-Film Probe Technique for Monitoring Shock-Wave Oscillations

Frederick W. Roos*
McDonnell Douglas Corporation, St. Louis, Mo.

A technique has been devised for sensing the instantaneous location of a normal shock wave as it oscillates about a mean position. Based on hot-film anemometer technology, the method involves a probe that is operated by a standard constant-temperature anemometer unit. Heat transfer from the probe's heated metal film is affected by the presence of a normal shock, which causes boundary-layer transition. As a consequence, the output voltage of the anemometer unit varies according to the location of the shock along the metal film. Sensitivity of the shock-position-sensing probe is shown to be in agreement with a simple two-dimensional flow model. The shock probe was employed during a transonic airfoil experiment to provide amplitude and frequency information on shock motions, and also to determine the relationship between shock motions and lift fluctuations in buffeting. These results have shown that the hot-film shock-position-sensing probe is a simple, effective instrument for studying the behavior of normal shock waves in unsteady flow.

Nomenclature

C = electrical/mechanical energy conversion factor
C_p = airfoil trailing edge pressure coefficient
c = airfoil chord
c_l = airfoil section lift coefficient
c_m = spanwise bending moment of airfoil
E = anemometer output voltage
f = frequency
i = probe heating current
k = thermal conductivity of air
M_∞ = freestream Mach number
Nu_{lam} = laminar Nusselt number, Eq. (2)
Nu_{turb} = turbulent Nusselt number, Eq. (3)
$q(x)$ = rate of heat transfer per unit area
R = probe resistance
$R(x_s,c_l)$ = cross-correlation coefficient relating unsteady components of x_s and c_l,

$$R(x_s,c_l) = \frac{1}{x_s' c_l'} \lim_{T\to\infty} \frac{1}{T} \int_0^T x_s(t)\, c_l(t+\tau)\,dt$$

Re_x = Reynolds number based on length x, $U_\infty x/\nu$
T_∞ = freestream static temperature
T_f = local metal-film temperature
$\bar{T}_f$ = average metal-film temperature
T_r = recovery temperature, Eq. (4)
T^* = temperature for evaluation of gas properties, Eq. (7)
U_∞ = freestream flow speed
w = width of metal film
x = streamwise distance from nose of probe
x_o = virtual origin of turbulent portion of boundary layer
x_s = location of shock wave
x_1 = upstream end of metal film
x_2 = downstream end of metal film
α = temperature coefficient of resistance of metal film
ν = kinematic viscosity of air
ξ = length variable in turbulent boundary layer, $x-x_o$
$\rho(x)$ = resistance per unit length of metal film
τ = cross-correlation time delay
Φ_a = power spectral density of the variable $a(t)$
ω^* = dimensionless frequency, $2\pi fc/U_\infty$
$(\,)_i$ = value at known reference condition
$(\,)'$ = root-mean-square value of unsteady component of variable

Presented as Paper 79-0331 at the AIAA 17th Aerospace Sciences Meeting, New Orleans, La., Jan. 15-17, 1979; submitted Feb. 16, 1979; revision received June 20, 1979.

Index categories: Testing, Flight and Ground; Shock Waves and Detonations; Nonsteady Aerodynamics.

*Scientist, McDonnell Douglas Research Laboratories. Member AIAA.

Introduction

A NEW technique has been developed for sensing the instantaneous location of a normal shock wave as it oscillates about a mean position. The technique was developed for experimental studies of unsteady transonic airfoil aerodynamics associated with buffeting.[1] Buffeting of an airfoil in transonic flow results from the development of a sizable region of separated flow which, in turn, is related to the presence of a normal shock on the upper surface of the airfoil. The shock may produce the separation directly, the so-called shock-induced separation, or indirectly, by weakening the boundary layer and thereby promoting trailing-edge separation.[2] In either case, unsteady movement of the shock will affect the associated separation, contributing to the unsteady loads that result in buffeting. Conversely, flow fluctuations in the separated region can generate pressure waves that alter the shock strength and affect its position. The nature of this interaction between the shock and separation needs clarification for proper modeling of transonic airfoil buffeting flowfields. In addition, knowledge of the role played by unsteady shock wave motion may provide clues for alleviating buffeting.

All previous evidence of the relationship between shock-wave motion and transonic airfoil buffeting was indirect. Transonic airfoil shocks revealed by continuous-light schlieren or shadowgraph systems could be seen to fluctuate around a mean position. Unsteady surface pressure measured at a point in the vicinity of the shock showed step changes in pressure that indicated passage of the shock, and the chordwise extent of the rapid-pressure-rise region on a transonic airfoil in buffeting gave some indication of the chordwise range over which the shock moved. None of these indications resulted in a direct measurement of shock position, which is

required for correlation with surface pressure and lift force fluctuations; hence, a new technique had to be devised.

Development of Probe Technique

Two principal requirements were established for the new shock-position monitoring technique. First, the selected approach had to result in an analog voltage output that would vary linearly, or at least monotonically, with shock-wave location to cross-correlate the time-dependent shock position with other unsteady variables. Second, flow interference had to be minimized; in particular, no interference with the interaction between shock wave and boundary layer could be permitted.

Several candidate approaches were rejected. A method based on standard two-dimensional optical techniques (shadow, schlieren) was of questionable value because it could not specifically identify the chordwise location of the shock at the midspan station, where all the static and dynamic pressure measurements were made. Spanwise variation of the mean shock location had been observed in earlier two-dimensional airfoil tests,[3] and it was anticipated that there might also be spanwise phase variation of the shock movements. Airfoil-surface measurements were also eliminated because the local effects of the boundary layer and associated shock-induced separation might obscure the time-dependent location of the shock. Consideration was given to a light-scattering technique that would have involved a laser, extensive optics, a scanning prism, and associated processing electronics. However, this technique was felt to be sufficiently complicated to require an extended development effort, and consequently was abandoned.

Familiarity with hot-film anemometry suggested the possibility of developing a heat-transfer device based on hot-film anemometer technology. The concept that evolved led to design of the probe shown in Fig. 1. In operation, the probe is aligned with the flow. The upstream ends of the probe is a quartz rod of circular cross-section; to minimize flow disturbance, the nose of the rod was carefully ground to a tangent ogive configuration. A thin, platinum film was deposited on the cylindrical surface of the quartz rod; two lengthwise splits, on opposite sides of the rod, were cut into the metal film. The upstream ends of the two separate film segments were joined by a conducting band, and the down stream end of each film was connected to a lead wire that ran down the inside of the probe body to a contact pin in the base of the probe. This design was intended to produce an axial (and therefore streamwise) path for the probe heating current; in fact, the layout required that the heating current pass twice the length of the heated metal film. The operating principle of the shock-position-sensing probe involves the difference in heat transfer rates up- and downstream of the shock. With the probe located so that the mean position of the shock lies somewhere along the metal film, and with the film maintained at a constant average temperature (i.e., constant average resistance) by a standard constant-temperature anemometer

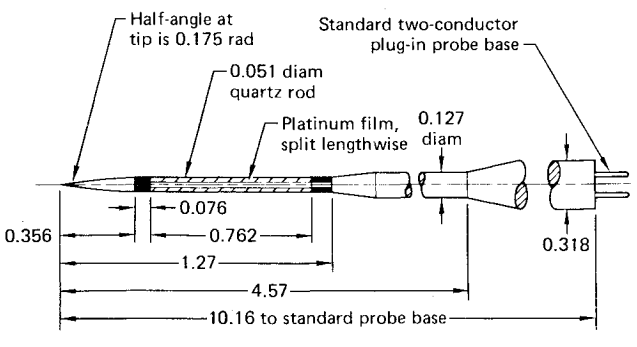

Fig. 1 Hot-film probe for sensing shock-wave oscillations.

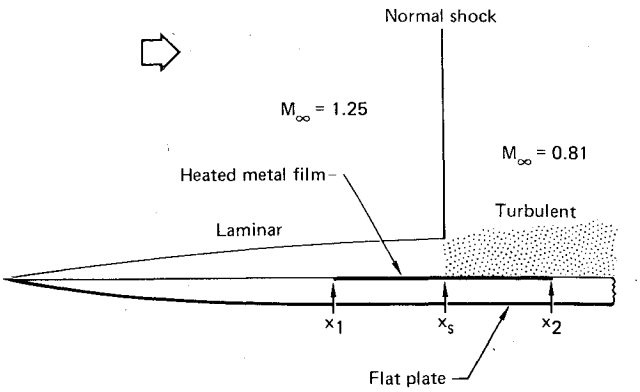

Fig. 2 Sketch of flow model used for probe heat-transfer analysis.

circuit, the heating current required to maintain that film temperature depends on the instantaneous location of the shock along the film.

A simple theoretical analysis of the probe operation was conducted to determine the validity of the concept. Several factors influence the relative heat transfer rates up- and downstream of the shock, the most important being the laminar/turbulent state of the boundary layer on the probe. Beginning with the assumption that the boundary layer is thin compared to the radius of the cylindrical probe body, the probe analysis was based on the simple two-dimensional model shown in Fig. 2. Additional assumptions included: no heat conduction through the quartz probe body; no heat conduction along the metal film; boundary-layer transition occurred immediately at the shock; and incompressible Nusselt numbers were valid. In terms of the Reynolds number,

$$Re_x = \frac{U_\infty x}{\nu} \tag{1}$$

the laminar and turbulent Nusselt numbers were taken to be[4]

$$Nu_{\text{lam}} = \frac{xq(x)}{k(T_f - T_r)} = 0.295 Re_x^{0.5}\left[1 - \left(\frac{x_1}{x}\right)^{3/4}\right]^{-1/3} \tag{2}$$

and[5]

$$Nu_{\text{turb}} \frac{\xi q(\xi)}{k(T_f - T_r)} = 0.0264 Re_\xi^{0.8} \tag{3}$$

where T_f is the temperature of the heated metal film and T_r is the recovery temperature,

$$T_r = T_\infty (1 + 0.169 M_\infty^2) \tag{4}$$

In Eq. (3), the length variable is $\xi = x - x_o$, where x_o is the virtual origin of the turbulent portion of the boundary layer (determined by the requirement that momentum thickness be continuous through the laminar/turbulent transition). In Eqs. (2) and (3), $q(x)$ is the heat flux per unit surface area; this heat is all generated electrically, so

$$q(x) = \frac{Ci^2 \rho(x)}{w} \tag{5}$$

where i is the heating current, w is the width of the metal film, and C represents the conversion factor between electrical and mechanical units; the resistivity of the metal film is

$$\rho(x) = \rho_i [1 + \alpha (T_f - T_i)] \tag{6}$$

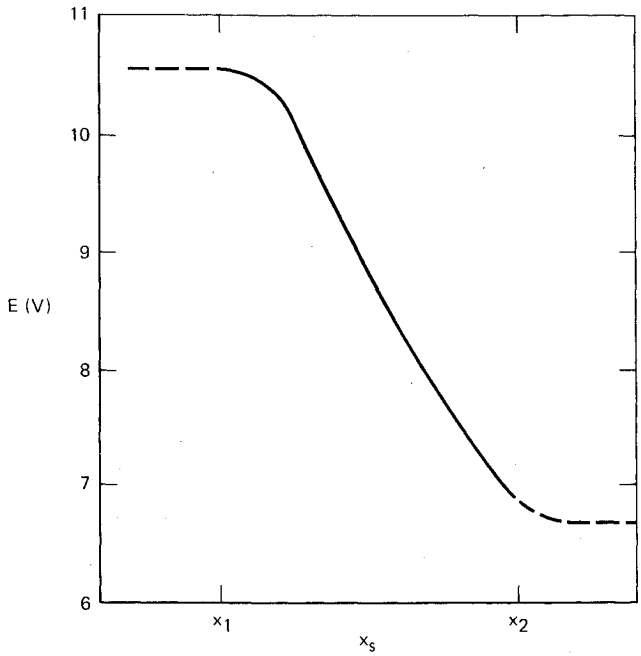

Fig. 3 Calculated shock-position-sensing probe output for typical flow conditions.

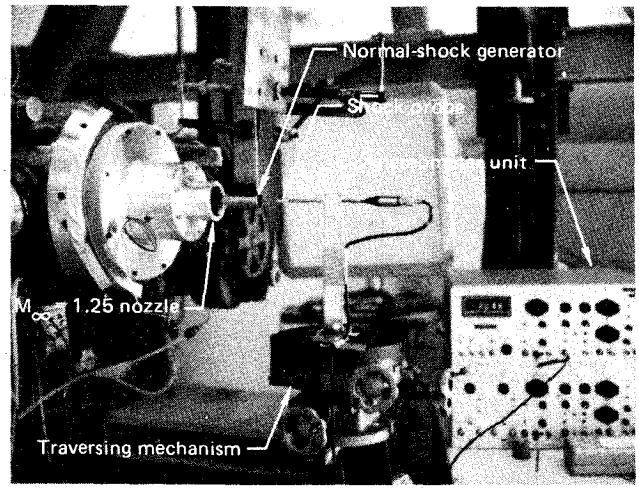

Fig. 4 Facility for test-calibrating shock-position-sensing probe.

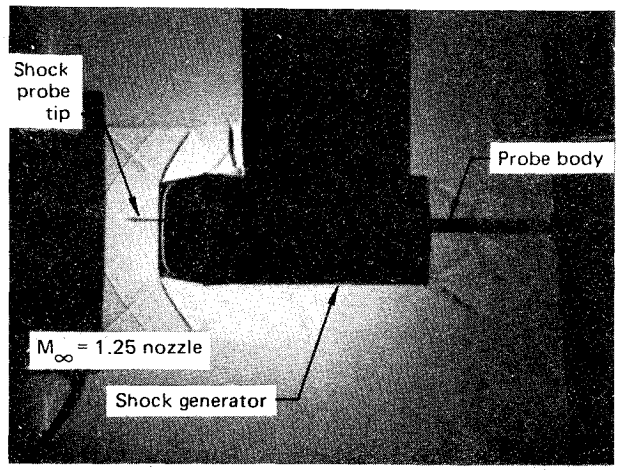

Fig. 5 Shadowgraph of flowfield during probe calibration.

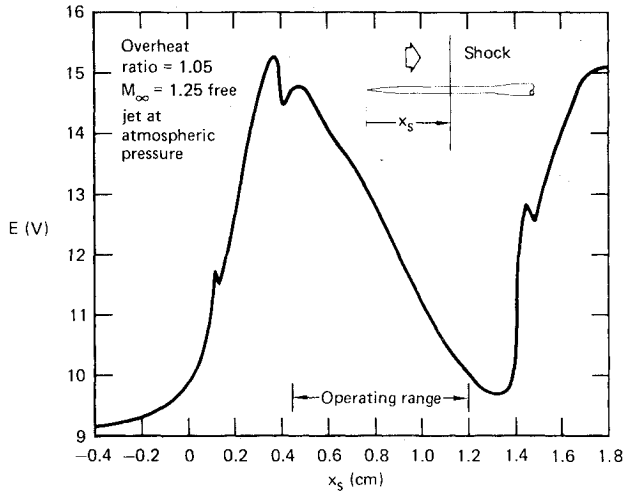

Fig. 6 Typical probe calibration curve.

where $(\ )_i$ denotes a measured reference condition and α is the temperature coefficient of resistance of the platinum film. Gas properties ν and k in Eqs. (1-3) are evaluated at the temperature[4]

$$T^* = 0.5(T_f + 0.56T_\infty + 0.44T_r) \tag{7}$$

Equations (1-7) can be combined and solved for T_f as a function of i and x_s for each portion of the boundary layer. The average metal-film temperature $\bar{T}_f$ is then found from

$$\bar{T}_f = \frac{1}{(x_2 - x_1)}\left[\int_{x_1}^{x_s} T_{f(\text{lam})}\,dx + \int_{x_s}^{x_2} T_{f(\text{turb})}\,dx\right] \tag{8}$$

Since the overall probe resistance R is given by

$$R = \int_{x_1}^{x_2} \rho(x)\,dx = R_i[1 + \alpha(\bar{T}_f - T_i)] \tag{9}$$

where $R_i = \rho_i(x_2 - x_1)$, $\bar{T}_f$ is directly related to the probe overheat ratio R/R_i. Practical overheat ratios were low (typically 1.05) because of the large cooling-surface area on the probe and limited available heating current in the anemometer unit used.

For the probe of Fig. 1 with an atmospheric normal shock of $M_\infty = 1.25$, the calculated probe response curve, E vs x_s (where E = anemometer output voltage, proportional to i), shown in Fig. 3 was produced. While not exactly linear, the system output voltage was definitely monotonic in, and sensitive to, x_s, and appeared to be easily linearizable with standard anemometer electronics.

Results

The test setup shown in Fig. 4 was used for experimental verification of the shock-position-sensing probe characteristics. A parallel-flow free jet with $M_\infty = 1.25$ was produced by an axisymmetric nozzle. The shock generator, a hollow cylinder with a sharp upstream edge, was placed coaxially within the jet, and the shock probe was then inserted along the axis of the shock generator until the probe tip penetrated the normal shock standing on the upstream end of the generator. Figure 5 is a shadowgraph of the flowfield during a probe calibration in the test facility. (The waves emanating from within the nozzle were produced by axisymmetric imperfections in the nozzle wall; the presence of these waves did not affect the test results.)

A typical probe test calibration curve showing anemometer output voltage E as a function of shock position is given in Fig. 6. The high sensitivity and near linearity of the output voltage are evident over the operating range of the probe (i.e.,

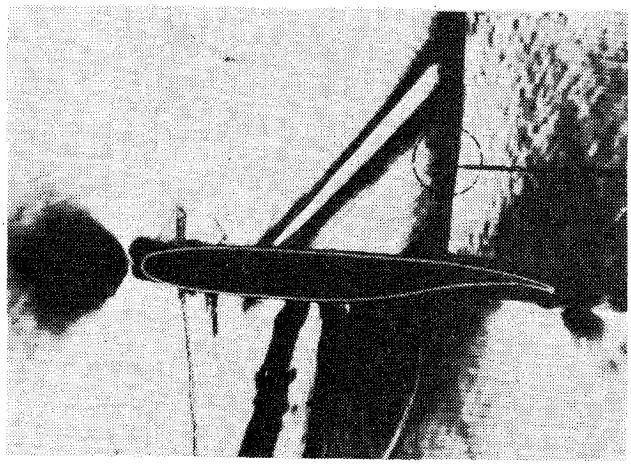

Fig. 7 Shock-position-sensing probe during transonic testing of supercritical airfoil.

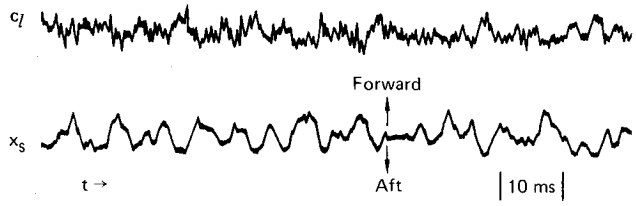

Fig. 8 Sample of shock motion data from airfoil test.

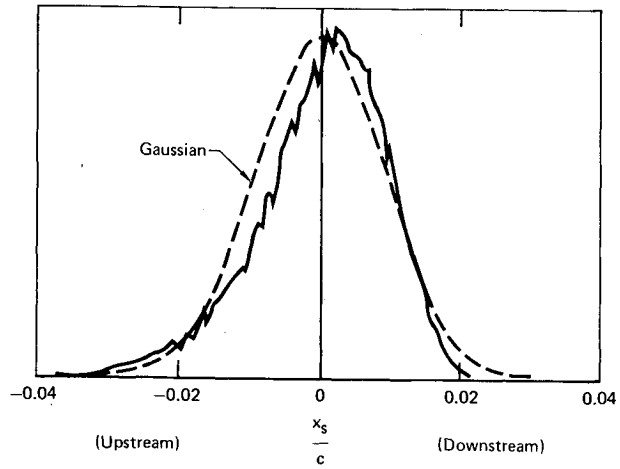

Fig. 9 Typical probability density function of shock wave displacement on a supercritical airfoil.

for the range of x_s over which the shock intersects the heated film), and the curve shape within this range is reasonably similar to the predicted response (Fig. 3). Unfortunately, two problems also appear in the calibration curve. One of these, the strange behavior of the calibration curve for $x_s > 1.4$ cm, is spurious, resulting from the probe having been moved sufficiently far upstream to interfere with the nozzle flowfield. The other problem, the rapid variation of E with x_s for $x_s < 0.5$ cm, is real, and is associated with the interaction of the shock with the local flowfield around the nose of the probe. When the probe is completely downstream of the shock ($x_s < 0$), the probe boundary layer is entirely laminar. As the probe penetrates the shock, i.e., as the shock moves downstream along the probe ($x_s > 0$), the shock causes the probe boundary layer to undergo transition, and consequently the heat transfer from the probe changes from the laminar rate to the turbulent rate as the shock moves aft along the upstream end of the probe. This phenomenon is unavoidable with the shock-position-sensing probe, and can lead to ambiguous data if shock movements being sensed by the probe extend beyond the probe's operating range. The potential for ambiguity can easily be alleviated by lengthening the probe tip to separate the two sections of the probe response curve.

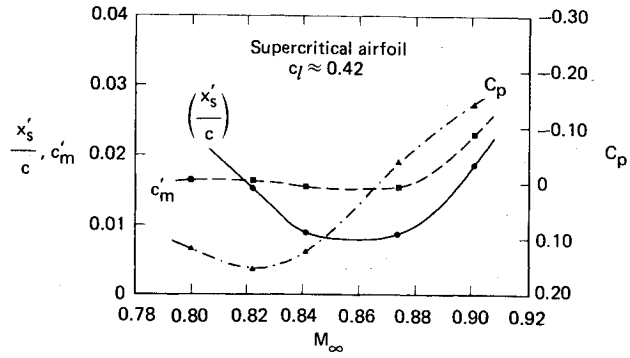

Fig. 10 Shock oscillation rms amplitude as a function of Mach number for a supercritical airfoil compared with trailing-edge pressure coefficient and rms wing bending moment.

The shock-position-sensing probe was employed in a recent series of transonic airfoil buffeting experiments.[6] The probe was mounted on a sting-supported, two-axis traversing unit that allowed remote positioning of the probe in both the streamwise and vertical directions. A spark schlieren photograph showing the probe in place during testing of a supercritical airfoil section is shown in Fig. 7. In order to calibrate the probe sensitivity for each flow condition, an in situ calibration procedure was used. Simply, the probe was traversed slowly in the streamwise direction while the dc output of the anemometer was recorded. As long as the extremes of the shock movement remained within the operating range of the probe, this procedure resulted in a valid calibration.

Figure 8 gives a sample of raw shock-motion data, along with simultaneously recorded fluctuation data. In the case shown, a definite correlation existed between upstream shock movement and decreasing lift. Examination of shock motion data in this raw form usually suffices to identify cases that have been affected by the probe output ambiguity described earlier, since the $x_s(t)$ signal is clipped and folded back on itself in these cases. The shock displacement record in Fig. 8 indicates that the frequency response of the shock-position-sensing probe system is good. This response was further investigated by employing the standard square-wave test used to evaluate the frequency response of hot-wire and hot-film anemometer probes. Although this test is artificial, as it involves electronically inserting a square-wave error signal into the feedback amplifier that controls the anemometer heating current, so that the system response time can be determined, it is generally accepted as a reasonably valid test. For the probe described here, under typical transonic airfoil flow conditions, the square-wave test indicated a cutoff frequency at about 5 kHz.

Unsteady shock displacement data from the airfoil tests were analyzed in several ways. For example, probability density distributions of shock position were determined for most cases. These distributions also helped to screen shock oscillation data that were distorted by the probe output ambiguity. An unambiguous case is shown in Fig. 9, where it is evident from the slight skewing of the probability density function that the shock moves upstream more easily than downstream (a consequence of the airfoil static pressure distribution).

An example of shock oscillation amplitude data (in root-mean-square form) is given in Fig. 10, where it is compared with trailing-edge pressure coefficient and unsteady spanwise bending moment, both of which are common indicators of buffet onset. The shock oscillation and bending moment

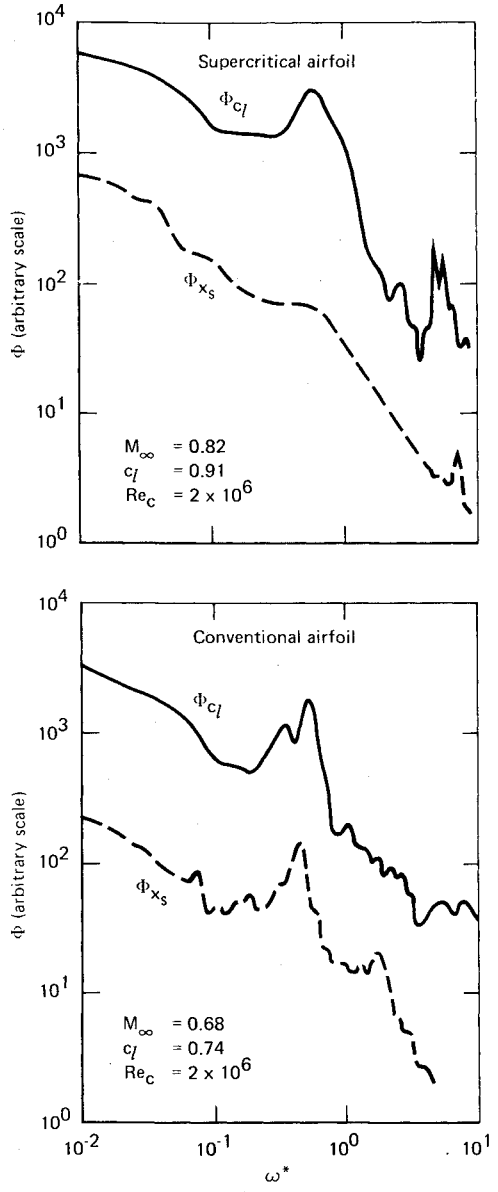

Fig. 11 Power spectra of shock oscillations on supercritical and conventional airfoils in transonic buffeting.

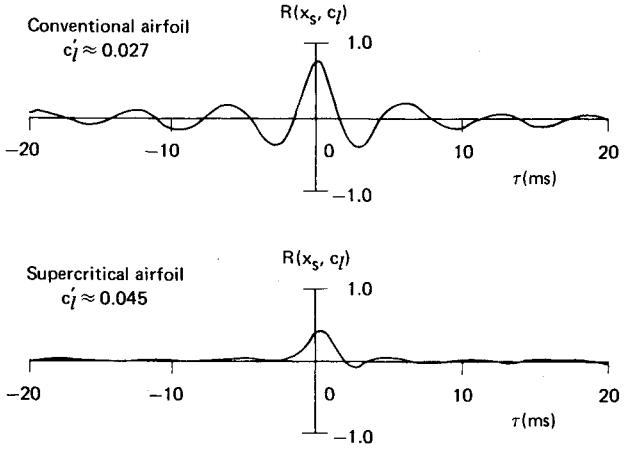

Fig. 12 Cross-correlation of shock oscillations and lift fluctuations for conventional and supercritical airfoils undergoing transonic buffeting.

amplitudes both begin to rise at $M_\infty \approx 0.88$, indicating buffeting development. The trailing-edge pressure coefficient (whose divergence results from trailing-edge flow separation) was not a good indicator of the onset of high-Mach-number buffeting for the supercritical airfoil.

Spectral analysis of the shock probe signals from airfoils in transonic buffeting showed that shocks on conventional and supercritical airfoils behave differently. Figure 11 compares shock oscillation power spectra for the two airfoil types. Shock oscillations on the conventional airfoil appear to be more tightly coupled to the lift fluctuations, as indicated by the strong spectral peaks that appear at a common frequency in the lift fluctuation and shock motion spectra for the conventional NACA 0012 airfoil. Although the unsteady lift power spectrum for the supercritical airfoil in buffeting shows a pronounced spectral peak similar to that of the conventional airfoil, there is no corresponding peak in the shock oscillation power spectrum for the supercritical airfoil. Further evidence of this difference in the extent of coupling of unsteady lift and shock motions between the two airfoil types is shown in Fig. 12, which gives cross-correlations of shock oscillations and lift fluctuations for both airfoils in heavy buffeting. The peak correlation is much greater for the conventional airfoil, demonstrating that the position of the shock wave, and the associated shock-induced flow separation, are more closely associated with the fluctuating lift for this airfoil than for the supercritical airfoil section.

Conclusions

A shock-position-sensing probe based on hot-film anemometer technology has been designed, and a technique for making real-time shock motion measurements has been demonstrated. The sensitivity of the shock probe has been found to agree reasonably well with predictions of a simple, two-dimensional heat transfer theory, the dominant mechanism of which is boundary-layer transition at the shock.

The shock-position-sensing probe technique was successfully used in transonic airfoil tests to provide valuable information on shock motions and their relationship to lift fluctuations during buffeting. These results have shown that the hot-film shock-position-sensing probe is a simple, effective instrument for studying the behavior of normal shock waves in unsteady transonic flow.

Acknowledgments

This research was conducted under the McDonnell Douglas Independent Research and Development Program in cooperation with the NASA Ames Research Center.

References

[1] Roos, F.W., "Surface Pressure and Wake Flow Fluctuations in a Supercritical Airfoil Flowfield," AIAA Paper 75-66, Pasadena, Calif., Jan. 1975.

[2] Pearcy, H.H., Osborne, J., and Haines, A.B., "The Interaction Between Local Effects at the Shock and Rear Separation—A Source of Significant Scale Effects in Wind-Tunnel Tests on Aerofoils and Wings," *Proceedings of the AGARD Conference on Transonic Aerodynamics*, AGARD CP-35, Sept. 1968.

[3] Hurley, F.X., "Measured Three-Dimensional Effects in Transonic Airfoil Testing," *AIAA Journal*, Vol. 13, Feb. 1975, pp. 250-252.

[4] Eckert, E.R.G. and Drake, R.M., Jr., *Heat and Mass Transfer*, 2nd ed., McGraw-Hill, 1959.

[5] Schlichting, H., *Boundary Layer Theory*, 4th ed., McGraw-Hill, 1960.

[6] Roos, F.W., "Some Features of the Unsteady Pressure Field in Transonic Airfoil Buffeting," AIAA Paper 79-351, New Orleans, Jan. 1979.